

Mechanisms of the Regulatory Effect of a Shenfu Injection Solution on NRF2-HO-1-GPX4 Ferroptosis Pathway to Alleviate Sepsis-Induced Myocardial Injury

ZHIYUAN LIU, QIAN WU, GUICAI YANG, DAN ZHANG, YI GU, HENG WANG¹, BO GU AND JUAN LIU*

Department of Critical Care Medicine, Qiannan Prefecture People's Hospital, ¹Qiannan Ethnic Medicine College, Duyun, Guizhou Province 558000, China

Liu *et al.*: Shenfu Injection Solution on Sepsis-Induced Myocardial Injury

Sepsis is a common infectious disease, and myocardial injury associated with sepsis is a major contributor to increased mortality. This work aimed to demonstrate the mechanisms by which a Shenfu injection solution regulates the nuclear factor erythroid 2-related factor 2, heme oxygenase-1, glutathione peroxidase 4, and ferroptosis pathway to alleviate sepsis-induced myocardial injury. Seventy-five C57BL/6J mice were selected and rolled into the following groups; control group, sham operation group (S1), positive control group (Y1), model group (M0), and Shenfu injection solution group (M1). After model establishment, each group received the corresponding treatment. Glutathione peroxidase 4, acetyl coenzyme A synthetize long chain family member 4, and polyunsaturated fatty acid coenzyme A levels were observed in the serum and myocardial tissues of the mice in each group. Experimental observations revealed that the glutathione peroxidase 4 expression was notably downregulated in the M0 group ($p < 0.05$), while acetyl coenzyme A synthetize long chain family member 4 and polyunsaturated fatty acid coenzyme A was greatly upregulated, accompanied by a noticeable increase in myocardial injury ($p < 0.05$). In contrast, glutathione peroxidase 4 was markedly upregulated ($p < 0.05$), while acetyl coenzyme A synthetize long chain family member 4 and polyunsaturated fatty acid coenzyme A level was drastically downregulated ($p < 0.05$) in the M1 group, leading to a remarkable reduction in myocardial injury. Shenfu injection solution can alleviate sepsis-induced myocardial injury by regulating the nuclear factor erythroid 2-related factor 2/heme oxygenase-1/glutathione peroxidase 4 ferroptosis pathway, downregulating acetyl coenzyme A synthetize long chain family member 4 and polyunsaturated fatty acid coenzyme A level, and upregulating glutathione peroxidase 4 level.

Key words: Shenfu injection solution, nuclear factor erythroid 2-related factor 2/heme oxygenase-1, glutathione peroxidase 4, sepsis, myocardial injury

Sepsis is a severe infectious disease characterized by clinical manifestations such as high fever, tachycardia and rapid respiration. It can cause severe systemic inflammatory response in patients and is one of the leading causes of postoperative mortality in critically ill patients^[1]. According to statistics, the global mortality rate of sepsis patients is as high as 10 %, and there are approximately 5 million cases of sepsis in China each year, with a mortality rate of up to 30 % among these patients^[2,3]. Severe sepsis can lead to postoperative organ dysfunction, including the heart, and sepsis-induced myocardial injury is a common complication in septic patients^[4]. In clinical research both domestically and

internationally, sepsis-induced myocardial injury has emerged as a crucial factor affecting patient survival time and prognosis. Hence, the search for therapeutic approaches that can alleviate sepsis-induced myocardial injury holds notable clinical significance.

In recent years, research on the treatment of sepsis-induced myocardial injury has attracted increasing

This is an open access article distributed under the terms of the Creative Commons Attribution-NonCommercial-ShareAlike 3.0 License, which allows others to remix, tweak, and build upon the work non-commercially, as long as the author is credited and the new creations are licensed under the identical terms

Accepted 11 September 2023

Revised 24 December 2022

Received 15 January 2022

Indian J Pharm Sci 2023;85(5):1388-1397

*Address for correspondence

E-mail: 45161441@qq.com

attention. Several studies have demonstrated that the adoption of antioxidants, vitamins and hypertonic solutions can alleviate sepsis-induced myocardial injury. The antioxidant function of puerarin has been confirmed in many studies. In a study investigating the role of puerarin-induced Adenosine Monophosphate activated Protein Kinase (AMPK)-mediated iron removal signaling in protecting against myocardial injury, it was found that puerarin exerted an inhibitory effect on Lipopolysaccharide (LPS)-induced myocardial injury. Puerarin promoted the upregulation of Glutathione Peroxidase 4 (GPX4) and ferritin protein levels, while notably downregulating the Acetyl Coenzyme A Synthetase Long Chain Family Member 4 (ACSL4), Transferrin Receptor (TFR), and cardiac iron content. Furthermore, the protein levels of GPX4 and ferritin were downregulated after the addition of the iron-removing activator compound erastin^[5]. These findings indicate that ferroptosis may be a potential mechanism contributing to septic myocardial injury. Ferroptosis is a form of cell death resulting from iron-dependent cellular damage caused by iron depletion and is distinct from apoptosis, autophagy-related programmed cell death, and necrosis, exhibiting a strong dependence on iron^[6]. Cell death resulting from iron depletion occurs due to iron-dependent lipid peroxidation within the cells, leading to a decrease in the expression levels of antioxidant factors, including glutathione and GPX4. GPX4 is capable of converting the peroxide bond in lipid peroxides into a hydroxyl group, thereby rendering the lipid peroxides inactive^[7]. Decreased expression and activity of GPX4 diminish the cell's ability to counteract oxidative stress, resulting in the accumulation of lipid peroxides and triggering oxidative cell death. Unlike apoptosis, during the process of ferroptosis, there are no membrane swellings, nuclear fragmentation, cell shrinkage or chromatin condensation. Nevertheless, mitochondrial shrinkage and an increase in lipid peroxides can be observed^[8]. During the process of iron depletion-induced cell death, inhibitors of programmed cell death and autophagy have no effect on inhibiting ferroptosis. Nevertheless, studies have found that this process can be inhibited by iron chelators, indicating the iron dependence of cell death through iron depletion^[9]. Ferroptosis has been implicated in various oxidative damage-related pathologies,

including acute kidney injury, neurotoxicity, viral hepatitis, myocardial injury and sepsis^[10-12]. Moreover, researchers both domestically and internationally are exploring novel therapeutic approaches. Recent studies have discovered that the Nuclear Factor Erythroid 2-Related Factor 2 (Nrf2) Heme Oxygenase-1 (HO-1)-GPX4 ferroptosis pathway is a promising treatment for Acute Liver Injury (ALI). In *in vitro* studies, it was found that Maresin 1 (MaR1) inhibited cell viability reduction induced by LPS and erastin, and improved the expression of Nrf2/HO-1/GPX4^[13]. Nrf2 and HO-1 are major antioxidant proteins that can inhibit the generation of reactive oxygen species through transcriptional regulation within cells. GPX4 is an antioxidant enzyme that plays a protective role in preventing oxidative damage to cells. Nrf2, HO-1 and GPX4 can collaborate to exert significant protective effects in ALI. The Shenfu injection is derived from the traditional Chinese medicine formula Shenfu decoction and primarily contains ginsenosides and water-soluble alkaloids. In numerous studies, Shenfu injection has been found to possess antioxidant properties, such as scavenging reactive oxygen species and inhibiting lipid peroxidation. Additionally, it has demonstrated effects in combating ischemia and hypoxia. In pharmacological, clinical and animal studies, it has been observed that Shenfu injection can enhance myocardial cell contractility, protect myocardial cells from ischemia-reperfusion injury, and inhibit the generation of lipid peroxides. Shenfu injection achieves these effects by activating the serine/threonine kinase AKT/Glycogen Synthase Kinase-3 beta (GSK-3 β) pathway, thereby alleviating cardiac dysfunction, preventing inflammatory damage, and reducing myocardial cell apoptosis in patients with septic cardiomyopathy^[14]. Moreover, ferroptosis, a newly discovered pathway of cell death, has been implicated in various conditions such as hypoxia, ischemia, benign or malignant tumors, and infectious diseases. Hence, investigating this novel therapeutic approach holds significant importance in elucidating the pathogenesis of septic cardiomyopathy.

Hence, exploring therapeutic approaches that can alleviate septic cardiomyopathy is currently a focal point in clinical research, with the Nrf2-HO-1-GPX4 ferroptosis pathway being one of the latest areas of investigation. Hence, this article

will primarily focus on the discussion of the mechanisms by which Shengfu injection regulates the Nrf2-HO-1-GPX4 ferroptosis pathway to mitigate septic cardiomyopathy and its potential clinical adoptions.

MATERIALS AND METHODS

Research materials:

This study employed 75 C57BL/6J mice (Jiangsu Jicui Yaokang Biotechnology Co., Ltd.) for experimentation. The mice had an average age of (6-8) w and an average weight of (18-24) g. Upon procurement, the mice were housed in our laboratory animal facility, with five mice per cage. The facility maintained a temperature of 25°, a humidity of 60 %, and a 12 h light-dark cycle synchronized with the external environment. The mice were provided with *ad libitum* access to food and water. Following 1 w of acclimatization in the housing facility, the mice were subjected to the experimental procedures.

Establishment, grouping and administration of animal models:

A total of 75 C57BL/6J mice were assigned into five groups; The Control (C1) group, Sham (S1) operation group, Positive control (Y1) group, Model (M0) group, and Shenfu injection treatment (M1) group, with 15 mice in each group. Except for the C1 and S1 groups, the Cecal Ligation and Puncture (CLP) surgery was performed to establish a mouse model of sepsis-induced acute myocardial injury (Creatine Kinase-Myocardial Band (CK-MB) >50 U/l). The M1 group received 1 ml of Shenfu injection *via* tail vein injection, while the Y1 group received 1 ml of dexamethasone solution (4 mg/ml) *via* tail vein injection. The remaining groups were administered an equivalent volume of normal saline. Injections were administered for every 10 h. The mice were monitored for mortality rates up to 10 d, and their body weights were measured before and after the experiment.

Model establishment: Forty-five mice were randomly selected to establish the sepsis model. The mice were fasted for 12 h prior to the CLP surgery, with access to water. Anesthesia was induced by injecting 0.1 ml/20 g of 8 % chloral hydrate solution into the mouse's abdominal cavity. The effectiveness of anesthesia was confirmed when the mouse showed no resistance when its tail

was lifted. The abdominal fur of the mouse was sterilized with alcohol swabs and excess fur was removed using scissors. The mouse's abdomen was longitudinally incised by 2-3 cm using a sterilized or autoclaved surgical blade, successively cutting through the skin, abdominal muscle layer, and entering the abdominal cavity. The location of the cecum was identified, and the cecum was carefully isolated and exteriorized, taking care to avoid damaging the surrounding blood vessels. A ligature was placed 2 cm proximal to the terminal end of the cecum using a no. 1 suture, and the cecum was punctured twice at the distal end of the ligature using an 18 gauge needle. Subsequently, the cecum was placed back into the abdominal cavity, and the incision was disinfected and sutured, sequentially suturing the muscle layer and skin of the abdomen. After completion of the surgery, 1 ml/20 g of normal saline was subcutaneously injected to reawaken the mice. The entire surgical procedure was completed within 15 min.

The S1 group underwent an abdominal incision procedure on the mice. After the abdominal cavity was opened and the cecum was located, the cecum was gently pulled out and the intestines were manipulated within the abdominal cavity. Subsequently, the cecum was placed back into the abdominal cavity without ligation or puncture.

Model selection:

At 6 h and 18 h before and after the surgery, blood samples of 0.5 ml were collected from the mice *via* the retro-orbital sinus and placed in Ethylenediaminetetraacetic acid (EDTA) anticoagulant tubes. The tubes were then centrifuged at 3000 rpm for 15 min at 4°, and the supernatant was carefully collected and stored for further analysis. The samples were stored at -80° until measurement of CK-MB and cardiac Troponin I (cTnI) levels.

Staining and immunohistochemistry of tissue sections:

The cardiac tissue from each group of mice was fixed using 4 % paraformaldehyde and subsequently embedded in paraffin for sectioning. Paraffin sections of the cardiac tissue were then subjected to Hematoxylin and Eosin (HE) staining, and immunohistochemically analysis. This allowed for the evaluation of pathological changes in the cardiac tissue as well as changes in the expression

levels of GPX4, ACSL4 and Polyunsaturated Fatty Acyl-CoA (PUFA-CoA) within the cardiac tissue.

Enzyme Linked Immunosorbent Assay (ELISA)

method:

ELISA method was used for determining the levels of oxidative stress products in the serum of mice in each group. The levels of Glutathione (GSH), Malondialdehyde (MDA), Reactive Oxygen Species (ROS), and Reactive Nitrogen Species (RNS) in mouse serum were measured according to the instructions provided with the ELISA kits. These measurements were used to evaluate the levels of lipid peroxidation in the mice from each group.

Reverse Transcription-quantitative Polymerase Chain Reaction (RT-qPCR) and Western Blot (WB) detection:

1 ml of serum was collected from each group of mice 24 h after administration for the extraction of total Ribonucleic Acid (RNA) and protein. The expression levels of key targets GPX4, ACSL4 and PUFA-CoA mRNA and protein related to ferroptosis were examined. RT-qPCR was performed. One eppendorf tube containing 1 ml of serum was mixed with 1 ml of Trizol reagent. Total RNA was extracted using the Trizol method, and after extraction, the concentration and purity of the RNA were measured. Then, the RNA was reverse transcribed into complementary Deoxyribonucleic Acid (cDNA), and the expression levels of GPX4 messenger RNA (mRNA), ACSL4 mRNA, and PUFA-CoA mRNA were quantified using RT-qPCR. The reaction parameters were as follows; denaturation at 90°-95° for 30 s, annealing at 55° for 30 s, extension at 72° for 30 s, with a total of 30 cycles. The extension step at 72° was performed for 10 min. The reaction system was 20 µl, and Glyceraldehyde 3-Phosphate Dehydrogenase (GAPDH) was set as the internal reference gene. The primers for the internal reference gene were as follows; forward 5'-CTGGAGAAACCTGCCAAGTATG-3' and reverse 5'-GGTGAAGAATGGGAGTTGCT-3'.

WB was also performed. Serum collected from the mice was utilized. The protein concentration was determined using the Bicinchoninic Acid (BCA) assay according to the instructions of the BCA protein assay kit. Sodium Dodecyl Sulphate-

Polyacrylamide Gel Electrophoresis (SDS-PAGE) gel was prepared, and the collected proteins were separated by gel electrophoresis. Subsequently, the proteins were transferred to a membrane, followed by washing the membrane with Tris-Buffered Saline with Tween 20 (TBST) buffer. A 5 % skim milk solution was applied for blocking, and after 30 min, the primary antibody was applied and incubated at 4° overnight on a shaker. The membrane was then washed with TBST thrice, followed by incubation with the secondary antibody at 25°. After the membrane was washed again, the protein bands were visualized using an infrared imaging system, and the grayscale values were analyzed.

Laser copolymerization:

Observation of GPX4, ACSL4 and PUFA-CoA levels in myocardial tissue of mice in each group by laser copolymerization. The paraffin-embedded sections of mouse myocardial tissue were placed in an oven and baked at 55° for 2.5 h to remove the paraffin and dehydrate the sections. The sections were then rinsed, fixed and rinsed again. They were treated with 0.2 % Triton X-100 to achieve tissue transparency. The sections were incubated with the primary antibody, blocked and incubated overnight at 4°. The next day, after washing, the sections were incubated with the secondary antibody. Nuclei staining was performed using 4,6-Di-Amidino-2-Phenylindole (DAPI) dye. The levels of GPX4, ACSL4 and PUFA-CoA in the myocardial tissue of each group of mice were observed.

Statistical processing:

Using Statistical Package for the Social Sciences (SPSS) 26.0, measurement data were recorded as mean±standard deviation. The significance was analyzed using t-tests, and intergroup comparisons were conducted using one-way analysis of variance. Differences were considered statistically significant when $p < 0.05$.

RESULTS AND DISCUSSION

The results of the analysis are illustrated in fig. 1 and fig. 2. Before modeling, CK-MB and cTnI levels differed inconsiderably among the groups. Nevertheless, after modeling, the serum levels of CK-MB isoenzyme in the M0 group were drastically increased vs. the S1 group, and cardiac troponin cTnI was also greatly elevated ($p < 0.05$). When comparing the M1 group with the M0 group,

the serum CK-MB levels in the mice were markedly elevated, while the serum cTnI levels were notably reduced ($p < 0.05$).

The results showed that the GSH in the M0 group mice was dramatically decreased relative to the S1 group, while the levels of MDA, ROS and RNS were markedly increased. In contrast, the M1 group mice exhibited a prominent increase in GSH vs. the M0 group, while the levels of MDA, ROS and RNS were greatly decreased relative to the S1 group as shown in fig. 3 and fig. 4.

The myocardial fibers in the C1 group mice were arranged neatly, with cells appearing plump and

elliptical, and the nuclei located centrally within the cells. The histological sections of the S1 group mice's myocardial tissue showed similar states to the C1 group, with no notable differences observed. In the M0 group mice, the myocardial fibers appeared swollen and disorganized, with the presence of vacuoles in the cytoplasm, loss of striations, increased cross-sectional area of the myocardium, and severe fibrosis. Nevertheless, in the Y1 group and the M1 group, the myocardial fibers appeared normal, showing restored orderliness, the presence of cytoplasmic vacuoles decreased, and the cross-sectional area of the myocardium reduced as shown in fig. 5.

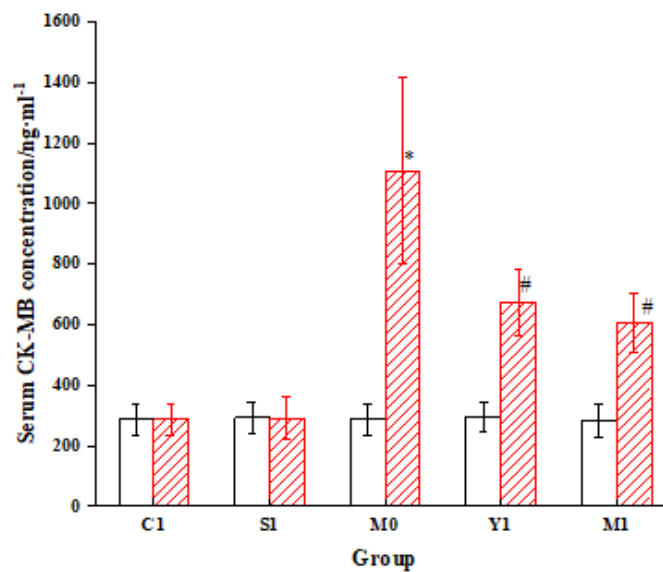


Fig. 1: Comparison of CK-MB levels of mice in each group before and after modeling
Note: * $p < 0.05$ vs. S1 group and # $p < 0.05$ vs. M0 group, (□): Before modeling and (▨): After modeling

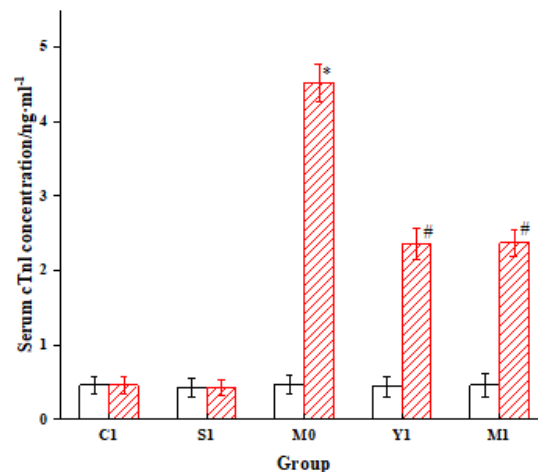


Fig. 2: Comparison of myocardial troponin cTnI levels of mice in each group before and after modeling
Note: * $p < 0.05$ vs. S1 group and # $p < 0.05$ vs. M0 group, (□): Before modeling and (▨): After modeling

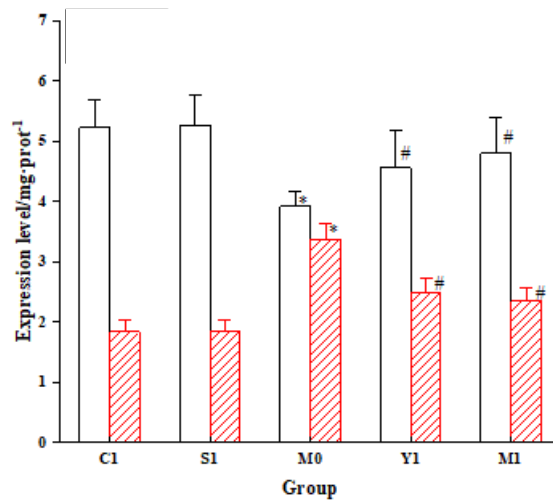


Fig. 3: Comparison of serum GSH and MDA levels in different groups of mice
 Note: *p<0.05 vs. S1 group and #p<0.05 vs. M0 group, (□): GSH and (▨): MDA

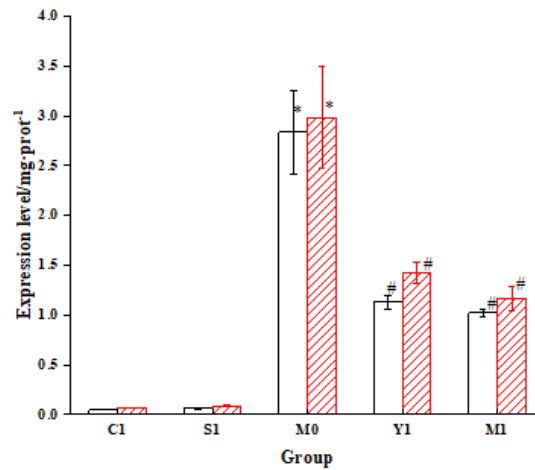


Fig. 4: Comparison of serum ROS and RNS levels in different groups of mice
 Note: *p<0.05 vs. S1 group and #p<0.05 vs. M0 group, (□): ROS and (▨): RNS

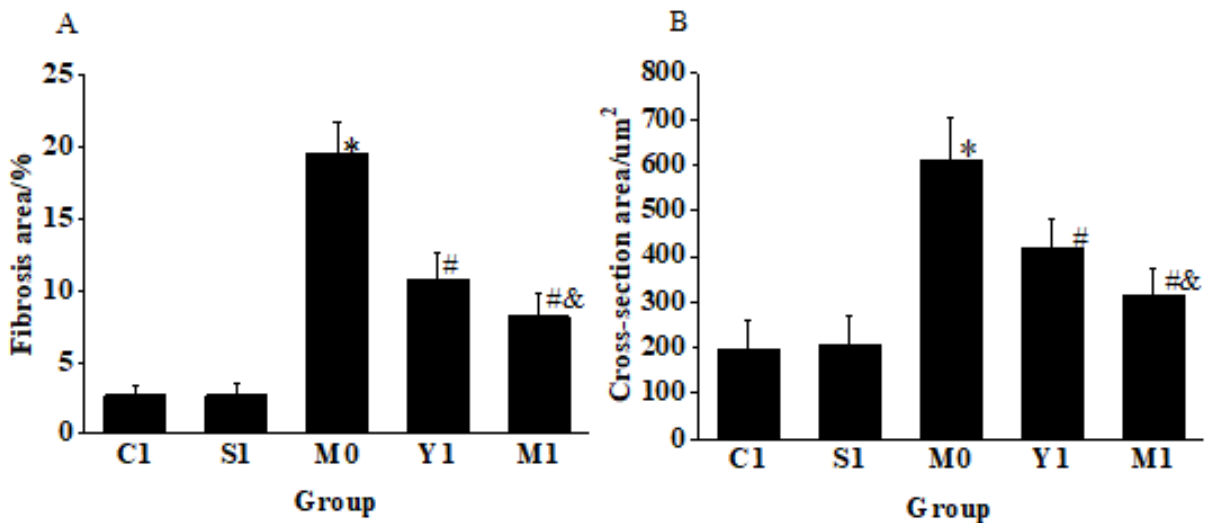


Fig. 5: The pathological characteristics of myocardial tissue in each group of mice, (A): Fibrotic area and (B): Cross-sectional area
 Note: *p<0.05 vs. S1 group; #p<0.05 vs. M0 group and #&p<0.05 vs. Y1 group

The results in fig. 6 revealed that the levels of GPX4 mRNA and PUFA-CoA mRNA in the myocardial tissue of the M0 group mice were drastically decreased vs. the S1 group. Conversely, the ACSL4 mRNA in the myocardial tissue of the M0 group mice was greatly increased relative to the S1 group ($p<0.05$). In the M1 group, the GPX4 mRNA and PUFA-CoA mRNA in the myocardial tissue were notably increased vs. the M0 group. Additionally, the ACSL4 mRNA in the myocardial tissue of the M1 group mice was greatly increased than the M0 group ($p<0.05$).

The research results (fig. 7) demonstrated that in comparison to the S1 group, the GPX4 level in the myocardial tissue of the M0 group mice was markedly decreased, while the ACSL4 was substantially increased ($p<0.05$). When comparing the M1 group with the M0 group, the GPX4 in the myocardial tissue of the M1 group mice

was greatly increased, whereas the ACSL4 was decreased ($p<0.05$).

The observation results in fig. 8 revealed that when comparing the M0 group with the S1 group, the fluorescence intensity of GPX4 and PUFA-CoA expression in the myocardial tissue of mice was greatly decreased (643.72 ± 96.43 vs. 1116.29 ± 104.41 ; 692.51 ± 98.26 vs. 1203.45 ± 123.53), while the fluorescence intensity of ACSL4 expression was markedly increased (1067.48 ± 154.25 vs. 713.28 ± 85.48) ($p<0.05$). When comparing the M1 group with the M0 group, the fluorescence intensity of GPX4 and PUFA-CoA expression in the myocardial tissue of mice was remarkably increased (967.25 ± 101.42 vs. 643.72 ± 96.43 and 985.35 ± 116.24 vs. 692.51 ± 98.26), while the fluorescence intensity of ACSL4 expression was decreased (865.24 ± 108.46 vs. $1,067.48\pm154.25$) ($p<0.05$) as shown in fig. 8.

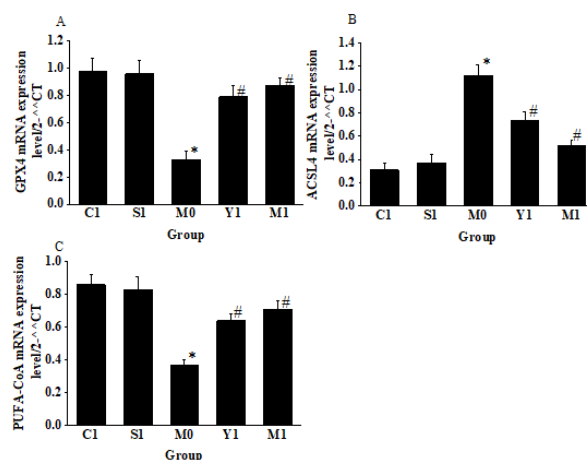


Fig. 6: Comparison of serum GPX4, ACSL4 and PUFA CoA mRNA levels in each group of mice, (A): GPX4 mRNA; (B): ACSL4 mRNA and (C): PUFA CoA mRNA

Note: * $p<0.05$ vs. S1 group and # $p<0.05$ vs. M0 group

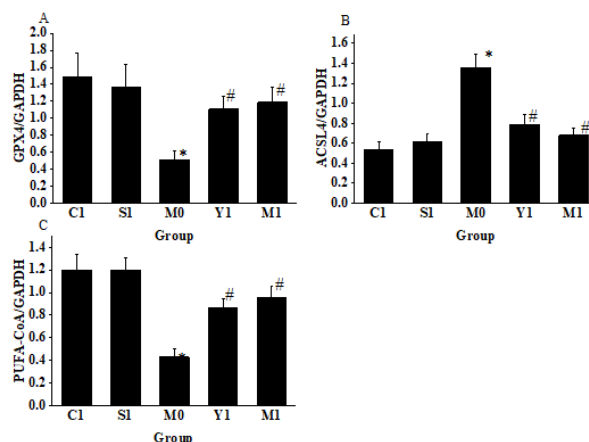


Fig. 7: Ferroptosis related proteins in the serum of mice in each group, (A): GPX4; (B): ACSL4 and (C): PUFA CoA

Note: * $p<0.05$ vs. S1 group; # $p<0.05$ vs. M0 group

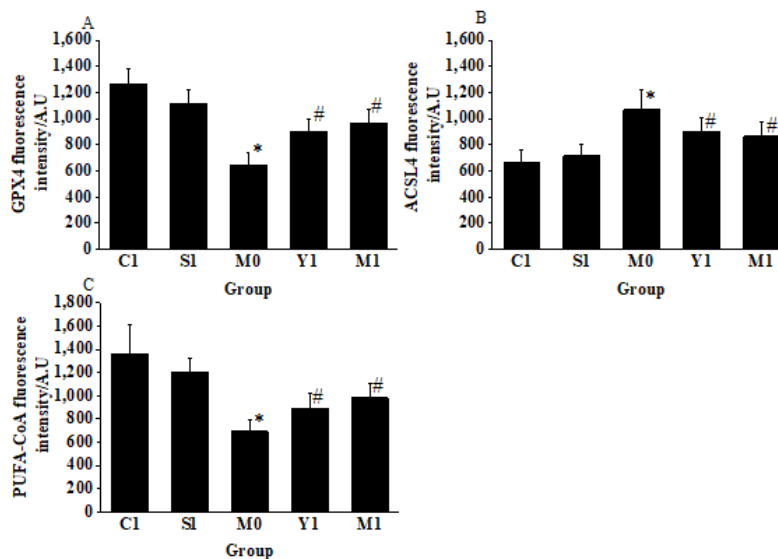


Fig. 8: Comparison of the expression of ferroptosis related proteins in the myocardial tissue of mice in each group. (A): GPX4; (B): ACSL4 and (C): PUFA CoA

Note: * $p < 0.05$ vs. S1 group and # $p < 0.05$ vs. M0 group

Pyogenic myocarditis is a severe complication of sepsis, directly associated with a high mortality rate^[15]. Enhanced oxidative stress response is a major characteristic of ferroptosis. Increasing evidence suggests that ferroptosis may be a potential mechanism underlying myocardial injury in pyogenic myocarditis. Studies have shown that Shenfu injection has a good clinical efficacy in the treatment of sepsis, with pinealtonin, ginsenoside Rf, ginsenoside Re, and cantharidin identified as key active components of Shenfu injection for sepsis treatment^[16]. Research has also found that Shenfu injection is effective in improving immune function in septic patients^[17,18], reducing septic lung injury^[19] and improving the prognosis of septic patients^[20]. Furthermore, Shenfu injection can downregulate the Mitogen-Activated Protein Kinase (MAPK) and Extracellular Signal-Regulated Kinase (ERK) signaling pathways to decrease the release of inflammatory cytokines such as Tumour Necrosis Factor- α (TNF- α), reduce inflammatory response, and inhibit cell apoptosis^[21]. Both experimental and clinical studies have demonstrated that Shenfu injection can improve pulmonary vascular permeability, inhibit glycocalyx degradation, reduce fluid retention in septic shock patients, and enhance tissue perfusion during early volume resuscitation^[22]. A study investigating postoperative myocardial function in patients has shown that myocardial injury leads to increased levels of CK-MB, cTnI and Heart-type

Fatty Acid-Binding Protein (H-FABP)^[23]. Hence, in this work, the levels of CK-MB and cTnI were measured to screen for the septic myocardial injury model. Nevertheless, the mechanism by which Shenfu injection may inhibit pyogenic myocarditis through the regulation of the ferroptosis signaling pathway and oxidative stress factors remains unclear.

The Nrf2/HO-1/GPX4 pathway is recognized to play a crucial role in maintaining cellular homeostasis and preventing oxidative stress damage. It has been found that inhibiting the Nrf2/GPX4 pathway promotes iron overload and exacerbates doxorubicin-induced cardiomyopathy^[24]. This indicates the critical importance of inhibiting the Nrf2/GPX4 pathway for myocardial injury recovery. Following the occurrence of sepsis, the oxidative damage marker ROS accumulates and is expressed in large quantities, leading to more severe myocardial injury^[25]. Mitochondria are the main producers of ROS in cells. In the electron transport chain, oxygen is sequentially reduced to superoxide anions, hydrogen peroxide, and hydroxyl radicals. Each type of free radical tightly associates with respiratory chain enzymes to prevent leakage. The release of free radicals promotes numerous reactions, generating a series of additional ROS and RNS with varying potencies^[26]. Iron depletion is a newly discovered form of regulated cell death that depends on

iron and ROS regulation. It directly or indirectly affects the activity of GPXs under the induction of small molecules. The imbalance in redox state and excessive accumulation of ROS lead to lipid peroxidation, resulting in the disruption of cell membrane integrity^[27]. In this work, it was found that the ROS notably increased in mice with sepsis-induced myocardial injury, indicating the presence of inflammation in septic cardiomyopathy, which may be associated with oxidative stress response. GPX4, as an imperative antioxidant enzyme, plays a critical protective role inside the cells. Research has shown that sepsis can activate the ferroptosis pathway in the body, leading to downregulation of GPX4, resulting in cell apoptosis and oxidative damage^[28]. In this work, it was found that the intervention of Shenfu injection could restore the expression of GPX4 by modulating the Nrf2-HO-1-GPX4 ferroptosis pathway, thereby enhancing the intracellular antioxidant capacity and preventing septic cardiomyopathy. Additionally, ACSL4 and PUFA-CoA have also been shown to play crucial roles in the ferroptosis pathway. When GPX4 is downregulated, ACSL4 and PUFA-CoA can synergistically promote iron ion transfer and intracellular oxidative stress response, leading to lipid peroxidation and cell apoptosis^[29]. The intervention of Shenfu injection can suppress the expression of ACSL4 and PUFA-CoA, thereby reducing the likelihood of lipid peroxidation and apoptosis occurrence. Currently, it has been discovered that the Nrf2-HO-1-GPX4 ferroptosis pathway can improve acute myocardial ischemia. Treatment with electro acupuncture in a myocardial ischemia model showed a decrease in Fe²⁺ levels and ACSL4 expression, as well as an increase in GPX4 and ferritin heavy chain protein level^[30].

Furthermore, Shenfu injection can modulate the Nrf2-HO-1-GPX4 ferroptosis pathway to alleviate septic cardiomyopathy. Experimental observations revealed that the CK-MB, cTnI, MDA, ROS, RNS and ACSL4 were increased, while GSH and GPX4 were markedly decreased in the myocardial tissues of the M0 group mice vs. S1 group. The elevated levels of myocardial oxidative damage markers indicated an increased severity of myocardial injury, leading to the downregulation of GPX4 and the upregulation of ACSL4. In contrast, relative to the M0 group, the mice treated with Shenfu injection exhibited drastic upregulation of GPX4 and marked downregulation of ACSL4 and PUFA-

CoA, accompanied by a considerable reduction in the severity of myocardial injury. These findings suggest that Shenfu injection-mediated modulation of the Nrf2-HO-1-GPX4 ferroptosis pathway can alleviate septic cardiomyopathy. The mechanism of action by which Shenfu injection alleviates septic cardiomyopathy through the modulation of the Nrf2-HO-1-GPX4 ferroptosis pathway holds promising clinical adoption prospects. Further research can explore its pharmacological mechanisms and refine the methods and approaches for its clinical adoption.

Conflict of interests:

The authors declared no conflict of interests.

REFERENCES

1. Liu Y, Zhuang L, Chen C, Qi X, Ye S, Gu Z. Levosimendan protects cardiomyocytes from sepsis-induced inflammation, endoplasmic reticulum stress and cell death. *J Biol Regulat Homeost Agents* 2023;37(1):577-86.
2. Sun X, Dai Y, Tan G, Liu Y, Li N. Integration analysis of m6A-SNPs and eQTLs associated with sepsis reveals platelet degranulation and *Staphylococcus aureus* infection are mediated by m6A mRNA methylation. *Front Genet* 2020;11:7.
3. Zhou J, Tian H, Du X, Xi X, An Y, Duan M, *et al.* China Critical Care Clinical Trials Group (CCCCTG). Population-based epidemiology of sepsis in a sub district of Beijing. *Crit Care Med* 2017;5(7):1168-76.
4. Yu X, Wang Y, Yang D, Tang X, Li H, Lv X, *et al.* α 2A-adrenergic blockade attenuates septic cardiomyopathy by increasing cardiac norepinephrine concentration and inhibiting cardiac endothelial activation. *Sci Rep* 2018;8(1):5478.
5. Zhou B, Zhang J, Chen Y, Liu Y, Tang X, Xia P, *et al.* Puerarin protects against sepsis-induced myocardial injury through AMPK-mediated ferroptosis signaling. *Aging (Albany NY)* 2022;14(8):3617-32.
6. Li J, Li M, Li L, Ma J, Yao C, Yao S. Hydrogen sulfide attenuates ferroptosis and stimulates autophagy by blocking mTOR signaling in sepsis-induced acute lung injury. *Mol Immunol* 2022;141:318-27.
7. Imai H, Matsuoka M, Kumagai T, Sakamoto T, Koumura T. Lipid peroxidation-dependent cell death regulated by GPx4 and ferroptosis. *Curr Top Microbiol Immunol* 2017;403:143-70.
8. Fang J, Kong B, Shuai W, Xiao Z, Dai C, Qin T, *et al.* Ferroportin-mediated ferroptosis involved in new-onset atrial fibrillation with LPS-induced endotoxemia. *Eur J Pharmacol* 2021;913:174622.
9. Yao W, Liao H, Pang M, Pan L, Guan Y, Huang X, *et al.* Inhibition of the NADPH oxidase pathway reduces ferroptosis during septic renal injury in diabetic mice. *Oxid Med Cell Longev* 2022;2022:1193734.
10. Wang C, Yuan W, Hu A, Lin J, Xia Z, Yang CF, *et al.* Dexmedetomidine alleviated sepsis-induced myocardial ferroptosis and septic heart injury. *Mol Med Rep* 2020;22(1):175-84.

11. Wei XB, Jiang WQ, Zeng JH, Huang LQ, Ding HG, Jing YW, *et al.* Exosome-derived lncRNA NEAT1 exacerbates sepsis-associated encephalopathy by promoting ferroptosis through regulating miR-9-5p/TFRC and GOT1 axis. *Mol Neurobiol* 2022;59(3):1954-69.
12. Yin J, Li W, Yao W. Effects of Xinjierkang on Nrf2/HO-1 expression in viral myocarditis mice models. *Cell Mol Biol* 2020;66(5):137-41.
13. Yang W, Wang Y, Zhang C, Huang Y, Yu J, Shi L, *et al.* Maresin1 protect against ferroptosis-induced liver injury through ROS inhibition and Nrf2/HO-1/GPX4 activation. *Front Pharmacol* 2022;13:865689.
14. Zhao L, Jin L, Luo Y, Wang L, Li Y, Xian S, *et al.* Shenfu injection attenuates cardiac dysfunction and inhibits apoptosis in septic mice. *Ann Transl Med* 2022;10(10):597.
15. Beesley SJ, Weber G, Sarge T, Nikravan S, Grissom CK, Lanspa MJ, *et al.* Septic cardiomyopathy. *Crit Care Med* 2018;46(4):625-34.
16. Yuan H, Liu Y, Huang K, Hao H, Xue YT. Therapeutic mechanism and key active ingredients of Shenfu injection in sepsis: A network pharmacology and molecular docking approach. *Evid-Based Complement Altern Med* 2022;2022.
17. Jin S, Jiang R, Lei S, Jin L, Zhu C, Feng W, *et al.* Shenfu injection prolongs survival and protects the intestinal mucosa in rats with sepsis by modulating immune response. *Turk J Gastroenterol* 2019;30(4):364.
18. Zhang N, Liu J, Qiu Z, Ye Y, Zhang J, Lou T. Shenfu injection for improving cellular immunity and clinical outcome in patients with sepsis or septic shock. *Am J Emerg Med* 2017;35(1):1-6.
19. Xing Y, Cheng D, Shi C. Protective effect of Shenfu injection on the endothelium of severe sepsis by inhibiting CD11b⁺ cell paralysis induced by high mobility group protein B1. *Zhonghua Wei Zhong Bing Ji Jiu Yi Xue* 2020;32(6):696-701.
20. Xu C, Xia Y, Jia Z, Wang S, Zhao T, Wu L. The curative effect of Shenfu injection in the treatment of burn sepsis and its effect on the patient's immune function, HMGB and vWF. *Am J Transl Res* 2022;14(4):2428.
21. Li MQ, Pan CG, Wang XM, Mo X, Shi ZX, Xu JY, *et al.* Effect of the Shenfu injection combined with early goal-directed therapy on organ functions and outcomes of septic shock patients. *Cell Biochem Biophys* 2015;7(3):807-12.
22. Rui-Juan CH, Qing-Lin RU, Qiong WA, Fang TI, Jian WU, Xiang-Qing KO. Shenfu injection attenuates lipopolysaccharide-induced myocardial inflammation and apoptosis in rats. *Chin J Nat Med* 2020;18(3):226-33.
23. Wang C, Wang H, Wu H, Li R, Zeng Y, Song D. The clinical effect of dexmedetomidine on myocardial function in cardiopulmonary bypass heart valve replacement. *Acta Med Med* 2022;38:3899.
24. Wang Y, Yan S, Liu X, Deng F, Wang P, Yang L, *et al.* PRMT4 promotes ferroptosis to aggravate doxorubicin-induced cardiomyopathy *via* inhibition of the Nrf2/GPX4 pathway. *Cell Death Differ* 2022;29(10):1982-95.
25. Fei Q, Ma H, Zou J, Wang W, Zhu L, Deng H, *et al.* Metformin protects against ischaemic myocardial injury by alleviating autophagy-ROS-NLRP3-mediated inflammatory response in macrophages. *J Mol Cell Cardiol* 2020;145:1-3.
26. Milbourn HR, Toomey LM, Gavriel N, Gray CG, Gough AH, Fehily B, *et al.* Limiting oxidative stress following neurotrauma with a combination of ion channel inhibitors. *Discov Med* 2017;23(129):361-9.
27. Zhao WK, Zhou Y, Xu TT, Wu Q. Ferroptosis: Opportunities and challenges in myocardial ischemia-reperfusion injury. *Oxid Med Cell Longev* 2021;2021:9929687.
28. Qiongyue Z, Xin Y, Meng P, Sulin M, Yanlin W, Xinyi L, *et al.* Post-treatment with irisin attenuates acute kidney injury in sepsis mice through anti-ferroptosis *via* the SIRT1/Nrf2 pathway. *Front Pharmacol* 2022;13:857067.
29. Wang YM, Gong FC, Qi X, Zheng YJ, Zheng XT, Chen Y, *et al.* Mucin 1 inhibits ferroptosis and sensitizes vitamin E to alleviate sepsis-induced acute lung injury through GSK3 β /Keap1-Nrf2-GPX4 pathway. *Oxid Med Cell Longev* 2022;2022:2405943.
30. Jiang ZM, Zhang L, Liu L, Wang J, Cai RL, Hu L, *et al.* Electroacupuncture improves ischemic myocardial injury by activating Nrf2/HO-1 signaling pathway to inhibit ferroptosis in rats. *Zhen Ci Yan Jiu* 2023;48(5):461-7.